Simulation of soil fluidization around a pressurized leaking pipe using the material point method

Monzer, Ali; Murphy, John; Yerro, Alba; Faramarzi, Asaad; Chapman, David

DOI:
10.1061/9780784484050.038

Simulation of Soil Fluidization Around a Pressurized Leaking Pipe Using the Material Point Method

Ali Monzer[1]; John Murphy[2]; Alba Yerro[3]; Asaad Faramarzi[4]; and David Chapman[5]

[1]Ph.D. Candidate, Dept. of Civil Engineering, Univ. of Birmingham, Edgbaston, Birmingham, UK. E-mail: axm1369@student.bham.ac.uk
[2]Ph.D. Candidate, Dept. of Civil and Environmental Engineering, Univ. of California, Berkeley; Research Civil Engineer, U.S. Army Engineering Research and Development Center, Vicksburg, MS. E-mail: john.w.murphy@erdc.dren.mil
[3]Assistant Professor, Dept. of Civil and Environmental Engineering, Virginia Polytechnic Univ., Blacksburg, VA. E-mail: ayerro@vt.edu
[4]Associate Professor, Dept. of Civil Engineering, Univ. of Birmingham, Edgbaston, Birmingham, UK. E-mail: a.faramarzi@bham.ac.uk
[5]Professor, Dept. of Civil Engineering, Univ. of Birmingham, Edgbaston, Birmingham, UK. E-mail: d.n.chapman@bham.ac.uk

ABSTRACT

Underground buried pipes are extensively used in water and sewer networks to meet different domestic and agricultural needs. Underground water networks may suffer from leakage problems through cracks or holes. Pipe leakage can lead to economic, environmental, health, and safety consequences. Leakage from pipelines can induce soil fluidization due to the increase of pore water pressure in the region of the leak. The soil fluidization reduces the bearing capacity of the supporting ground, ultimately leading to the collapse of the ground and the buried utilities. In this study, the soil fluidization mechanism due to pressurized pipe leakage is numerically modeled with the Material Point Method (MPM). MPM represents the continuum with a set of integration points, so-called material points (MPs) that move attached to the media, carrying all the material information. Two MPM two-phase approaches are used to understand the soil-fluid interaction mechanisms associated with a leaking buried pressurized water pipe embedded in fully saturated sand. The single-point approach represents the saturated medium with one set of MPs; the double-point approach separately models the solid and the liquid phases using two sets of MPs. The capabilities of the two approaches to simulate the onset and evolution of soil fluidization are presented and discussed. Finally, the displacement field and failure mechanism around the leaking pipe are analyzed in terms of the soil porosity.

1. INTRODUCTION

Water loss due to pipe leakage is a major issue for various countries around the world, with a global leakage rate of 35% (Global Water Leakage Summit, 2008). Pipe leakage is caused by poor construction, deterioration, external loads, lack of maintenance, geological hazards, and seasonal soil variations. Severe consequences resulting from pipe leakage have been reported all over the world (Colombo and Karney, 2002). For example, the formation of underground cavities (van Zyl et al., 2013). Another consequence is soil fluidization which occurs when soil particles lose their interlocking forces and move freely with the pore fluid (Alsaydalani, 2010). Soil fluidization is the phenomenon in which soil particles turn into a viscous fluid or fluid-like state that is in contact with the fluid (Richards et al., 1990). Soil fluidization and cavity formation in the region of a leak results from fluid leaking from cracks, joints openings, and other forms of pipeline structural failure (Li, 2013). In the region of the

leakage, pore pressure increases and induces a reduction in effective stresses (eventually can become zero). The soil fluidization phenomenon is associated with a soil uplift mechanism and the formation of a fluidized zone in the vicinity of the leakage (Cui, 2013). The fluidized zone in which the soil is mobilized and moved with water extends from the leaking region towards the soil surface. This process results in a reduction of bearing capacity leading to surface subsidence. Thus, understanding the underground pipe leakage-soil interaction is an essential factor to maintain underground and surface infrastructure safety. Pipelines are most commonly buried underground, which hinders the ability to observe and wholly understand pipe leakage-induced fluidization of soil. Various laboratory studies have been conducted to study the soil fluidization mechanism around leaking pipes (Rogers et al., 2008; Teeluckdharry, 2017). These studies helped to define the soil fluidization mechanism. However, difficulties and uncertainties in the data acquisition inhibited these studies from determining essential factors for interpreting the soil-fluid behavior, including the soil effective stresses and fluidizing pressure. To gain full knowledge of the soil behavior and the transition to the post-fluidization process requires further study.

Considerable effort has also been deployed to numerically model the soil fluidization around a leaking pipe using different approaches. This includes FEM analyses conducted by Zhu et al. (2018) that investigated the effect of different water pressure, crack lengths and locations, and soil layering on the flow regime. From previous experimental work, it has been observed that once fluidization occurs, a localized cavity forms near the leak area that is characterized by large deformations. Due to the localized large soil displacements, FEM suffers from mesh tangling (Wang et al., 2015), and it is not capable of simulating the whole mechanism. Other methods are better suited for the simulation of large deformations. For example, Cui (2013) used the coupled Discrete Element Method-Lattice Boltzmann Method (DEM-LBM) to capture the inhomogeneities of granular particle behavior in the soil fluidization around a leaking pipe. However, for real-scale pipe leakage problems, DEM is computationally expensive.

In this analysis, the Material Point Method (MPM) is proposed to investigate the soil fluidization around leaking pressurized pipe because of its ability to simulate large deformations in multi-phase materials. The MPM was developed by Sulsky et al. (1994), and it has shown to be a powerful technique in various geotechnical and hydraulic fields, such as the study of granular flow (Więckowski, 2003; Yerro et al., 2014; Phuong et al., 2014). The MPM can model large deformations in multi-material and multi-phase problems (Bandara and Soga, 2015). It represents the continuum with a set of integration points, so-called material points (MPs) that move attached to the media, carrying all the material information. The main governing equations, generally the dynamic momentum balances, are solved at the nodes of a computational mesh that covers the whole computational domain. There are two distinct formulations for simulating the solid-fluid (two-phase) interaction in saturated porous media (Ceccato et al., 2018). The two-phase single-point approach, where one set of MPs is adopted (Zabala and Alonso, 2011), and the two-phase double-point approach that consists of two sets of MPs (Więckowski, 2003).

The objective of this paper is to show the present capabilities of the two MPM approaches to simulate the onset and evolution of soil fluidization around a leaking pipe. For the purpose of this study, the size of the orifice or crack is assumed relatively large to reduce the computational cost of the models. Advanced in/outflow Boundary Conditions (BCs) have been employed in the double-point approach to prescribing velocity-controlled inflow of material points (MPs) to the domain.

The paper is organized as follows. First, the basis of the two-phase MPM approaches is presented, followed by the description of the numerical models. Then, the results are presented and discussed. Finally, the conclusions are summarized in the end. All models

presented here are performed with an in-house version of the open-source Anura3D software (Anura3D, 2021).

2. BASIS OF THE MPM TWO-PHASE APPROACHES

2.1 Two-Phase Single-Point Approach

In the two-phase single-point formulation, the porous medium is simulated based on the macroscale continuum approach, where the saturated soil is defined by the solid skeleton kinematics using one set of MPs (Al-Kafagi, 2013). The total volume and properties of the two solid and liquid phases are represented in each MP. Following the Lagrangian approach of the solid movement, MPs travel connected to the solid skeleton, while the fluid movement is attached to the solid motion. In this formulation, each MP satisfies the solid mass conservation, but the liquid flow may alter the total mass. The two-phase single-point approach has proved an efficient technique for modeling geotechnical problems such as the slope collapse (Soga et al., 2016) and the CPT (Cone Penetration Testing) testing (Ceccato et al., 2016).

2.2 Two-Phase Double-Point Approach

The two-phase two-point MPM implementation (e.g., Więckowski, 2013; Martinelli and Rohe, 2015) simulates the soil-fluid interaction based on the volume fractions approach (Truesdell and Toupin, 1960). This mixture theory assumes that each point in a body's space consists of a finite number of particles that represent the mixture's constituents. In such a framework, each phase (i.e., solid and liquid) is defined by a separate set of Lagrangian MPs. The solid material points (SMPs) travel connected to the solid skeleton, and the fluid liquid material points (LMPs) move attached to the fluid. In contrast to the single-point approach, the double-point formulation fulfills both liquid and solid mass conservation (Ceccato et al., 2018). The LMPs can represent the pore water as well as the free water. Because of this, the porosity gradients can be large, and fluxes induced by this change cannot be neglected in the liquid mass balance. Additionally, a porosity threshold $n_{\max}$ is defined to distinguish between solid-like vs. liquid-like behavior. When a low porosity ($n < n_{\max}$) characterizes the saturated soil, the material (SMPs) is controlled by the effective stresses, and constitutive models used for granular soil can be used. When the porosity is large ($n > n_{\max}$), effective stresses in the SMPs are assumed equal to zero, and the Navier-Stokes equation is used to describe the liquid-like response of the mixture (Martinelli, 2016). In these circumstances, the SMPs behave as a viscous Newtonian fluid that is governed by an equivalent viscosity, assumed to be dependent on the volumetric concentration ratio of the solid phase in the saturated mixture (Beenakker, 1984).

3. NUMERICAL MODEL

The simulation of soil fluidization induced by a leaking pipe is conducted using the two MPM approaches considered in this study, i.e., two-phase single-point formulation and two-phase double-point formulation. The two-dimensional model used in each approach is presented in this section, where a fully submerged sand bed is connected to a pressurized inlet pipe through an orifice. As the aim of this research at this stage is to study the soil fluidization around the leaking pipe, only the orifice is modeled and not the whole pipe. This helps to simplify the model while reducing the computation time. The soil and water parameters used in the numerical model are listed in Table 1, which are extracted from the experiment conducted by Alsaydalani (2010).

3.1 Two-Phase Single-Point Model

In this section, the model designed to study the soil-fluidization around a leaking pipe using the two-phase single-point approach is presented (Figure 1). The soil bed is 500 mm in height and 1000 mm in length. An empty space is modeled at the top of the soil bed that allows the top vertical displacement of the material. The size of the empty space is chosen to be 100 mm, which is greater than the maximum expected displacement of the MPs at the surface. An orifice with a width of 100 mm is positioned in the middle of the soil base. Note that the size of the orifice is larger than previous experimental and numerical studies (Alsaydalani, 2010; Cui, 2013). This is selected to reduce the computational cost.

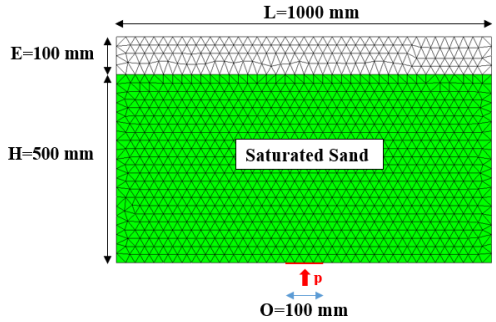

Figure 1: Discretised domain employed in the single-point modeled problem where p is the applied water pressure, H is the height, L is the length, O is the orifice, and E is the empty space.

A two-dimensional mesh comprising 2124 three-node triangular elements has been used as the computational grid. At the beginning of the simulation, three MPs are assigned within the filled elements. The elements have a nominal element size of 0.025 m (Figure 1). A homogeneous saturated soil layer is considered. The soil behavior is modeled using the Mohr-Coulomb elastic-perfectly plastic constitutive model (MC) that is simple and serves as a first-order model. Mohr-Coulomb is a failure criterion that is used to predict the shearing behavior of soil and thus the soil deformation. The water bulk modulus is decreased by 20 times with respect to optimize the computational time. This has an insignificant effect on the results as it is still large enough compared to the effective Young's modulus of the solid matrix. The intrinsic permeability (k) is assumed constant throughout the two-phase single-point simulation. All the material properties are extracted from the study conducted by Alsaydalani (2010) that are summarized in Table 1. Solid and liquid displacements on the left and right sides of the model are fixed in the horizontal direction, while the bottom boundary is fully fixed in both horizontal and vertical directions. A vertical fixity is also applied at the top of the model to avoid MPs leaving the mesh. A strain-smoothing algorithm is used to reduce the kinematic locking (Al-Kafaji, 2013). Stresses are initialized via an earth pressure coefficient at rest (K_0) procedure, and pore pressures are initially hydrostatic. The water leakage at the orifice is modeled by removing the vertical liquid fixity in the crack where excess water pressure is applied to the nodes. In each simulation, constant water pressure ranging from 5-15 kPa is applied at the orifice through the calculation.

Table 1: Material parameters of the model, equivalent for the silica sand and water (* parameters only required for the double-point formulation) (Alsaydalni, 2010).

Material Parameter	Symbol	Unit	Value
Initial porosity	n_0	–	0.34
Density soil	ρ_s	kg/m^3	2660

Water density	ρ_l	$\mathrm{kg/m^3}$	1000
Intrinsic permeability	k	$\mathrm{m^2}$	4.0×10^{-11}
Water bulk modulus	K_l	kPa	50000
Water viscosity	μ_d	kPa. s	8.905×10^{-7}
K_0-value	K_0	–	0.44
Effective Poisson ratio	ν'	–	0.3
Effective Young's modulus	E'	kPa	69000
Effective Cohesion	c'	kPa	0.1
Effective friction angle	ϕ'	degree	34
Dilatancy angle	ψ	degree	0
Tensile Strength	σ'	kPa	0.148
Soil grain diameter*	D_p	mm	0.9'
Maximum porosity*	n_{max}	–	0.45'

3.2 Two-Phase Double-Point Model

A similar problem is modeled using the two-phase double-point approach (Figure 2). In this case, the fluid flow is induced by applying a constant water flow through the orifice, and the in/outflow boundary conditions (BCs) introduced by Zhao et al. (2019) are used. For this reason, inflow and outflow zones are included in the model to allow the LMPs to enter and leave the computational. The length of the soil bed is 2,000 mm, which is larger than the one presented in Figure 1 to avoid BC effects during the evolution of fluidization (as discussed in the following section). In the inflow element (Figure 2, in green), LMPs are assigned with a prescribed velocity. When an inflow element is empty, new LMPs are added at the Gauss point location to refill the inflow elements. The outflow elements (Figure 2, in yellow) ensure a constant free water table (pressure zero at the water surface) by automatically removing those LMPs that enter the outflow zone. Water elements (Figure 2, in blue) represent those elements initially filled with LMPs representing free water. The saturated soil region (Figure 2, in purple) is initialized by placing both SMPs and LMPs to represent the two-phase media. The inflow velocities prescribed in the double-point are used to target the equivalent pressure as the single-point. Thus, both models of the two MPM approaches considered in this study are comparable despite the fact of using different boundary conditions.

The soil behavior is modeled using the Mohr-Coulomb elastic-perfectly plastic constitutive model (MC), and water is represented by the standard Newtonian compressible constitutive model. The material parameters (Table 1) and the orifice size (100mm) are the same as those used in the single-point approach. The intrinsic permeability (k) is set as a function of the diameter of the solid grains (D_p) and the solid porosity (n) with the Kozeny-Carman formula (Bear, 1972). In this formulation, the maximum porosity (n_{max}) is used as an additional parameter to differentiate between the solid and liquid state of the mixture. This parameter is determined based on the provided maximum void ratio from Alsaydalani's experiment (2010). The model is comprised of $3{,}510$ three-node triangular elements with an element size of 0.025 m. Six MPs per element (three LMPs and three SMPs) are initially assigned to the saturated soil domain, and six liquid MPs are assigned to the free water and inflow elements. Solid and liquid displacements are constrained in the normal direction and free in the longitudinal direction in the lateral boundaries. The bottom of the saturated soil region is fully fixed except for the orifice region that LMPs are allowed to move vertically. The effective stresses are initialized via K_0 procedure, and pore pressures are initially hydrostatic. The prescribed flow velocity ranges from 10^{-3} m/s to 10^{-2} m/s.

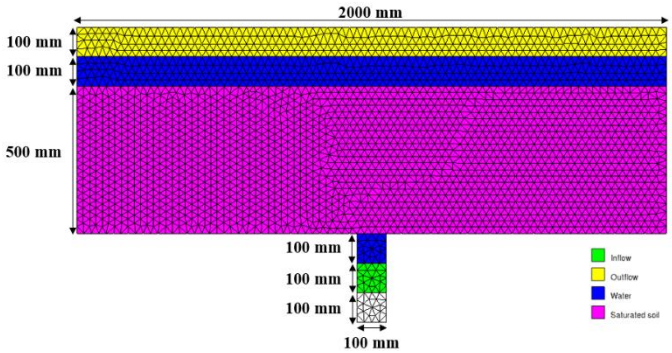

Figure 2: Discretised domain employed in the double-point modelled problem.

4. RESULTS AND DISCUSSION

This section presents and discusses the results obtained with the two-phase single-point and double-point MPM approaches.

4.1 Two-Phase, Single-Point Results

In this section, the results obtained with the single-point approach are presented. Figure 3 shows the excess pore water pressure distribution in the soil bed subjected to a 10 kPa in excess water pressure at a 100 mm orifice after 2s of simulation. It is shown that the pore pressure is highly accumulated in the vicinity of the orifice. This quickly dissipates, moving up the soil bed away from the pressure source.

Figure 4 presents the change in the excess pore water pressure after 2s of simulation at different heights in the soil bed for different applied water pressures (p= 5 kPa to 15 kPa). It is observed that the excess pore water pressure increases correspondingly with the increase in the applied pressure at the orifice. As the controlled water pressure is increased from 5 kPa to 14.5 kPa, the excess pore water pressure expands within the soil bed. Beyond these values, the excess pore water pressure at 25 mm above the orifice drops from a peak of 12.4 kPa to 11.2 kPa, corresponding to an applied pressure of 14.5 kPa and 15 kPa, respectively. However, an approximately steady state of the excess pore water pressure is noticed near the soil surface. This is due to the localized nature of the problem.

Based on the previous experimental (Alsaydalani, 2010) and numerical (Cui, 2013) studies, the onset of fluidization that occurred in the vicinity of the orifice is associated with a peak in excess pore water pressure that is attributed to the uplift mechanism of the soil bed above the pipe orifice. In the presented example, an applied pressure of 14.5 kPa results in a peak excess pore water pressure. Thus, 14.5 kPa is defined as the minimum pressure that is required for the onset of soil fluidization. This is followed by an abrupt drop in the excess pore water pressure in the vicinity of the orifice. Although the orifice size and the applied water pressure are not the same as in the previous studies, a consistent fluidization mechanism is recognized in this study with the single-point MPM approach. The MPM results agree well qualitatively with the previous experimental (Alsaydalani, 2010) and numerical (Cui, 2013; Li, 2013) solutions.

Figure 5 shows the soil vertical displacement after 2s of simulation for two different applied pressures (p=10 and 14.5 kPa). Displacements are relatively small (maximum of 0.15 mm) in the vicinity of the orifice before the onset of fluidization at an applied water pressure of 10 kPa (Figure 5a). These soil displacements increase at the onset of fluidization to 0.3 mm at an applied water pressure of 14.5 kPa (Figure 5b). The uplift mechanism in the soil bed is attributed to the peak in pore pressure where the soil is lifted in an upward direction above the orifice leading to the formation of the fluidized zone. The angle of the mobilized zone is 61° as drawn from the edge of the orifice to the soil surface along the boundary of the

distributed zone (Figure 5b). The inclination angle of the wedge is consistent with Alsaydalani (2010) and Cui (2013) that used the same soil parameters. In addition, the resulting angle is expected theoretically based on the angle of shear failure that is related to the angle of internal friction of the soil (34°), i.e. [45° + (34/2)] = 62°.

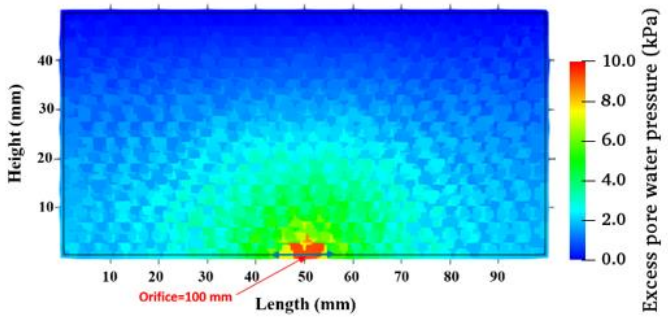

Figure 3: Excess pore water pressure distribution after 2s of simulation in a submerged soil bed based on MPM results where an excess water pressure (10 kPa) is imposed at an orifice.

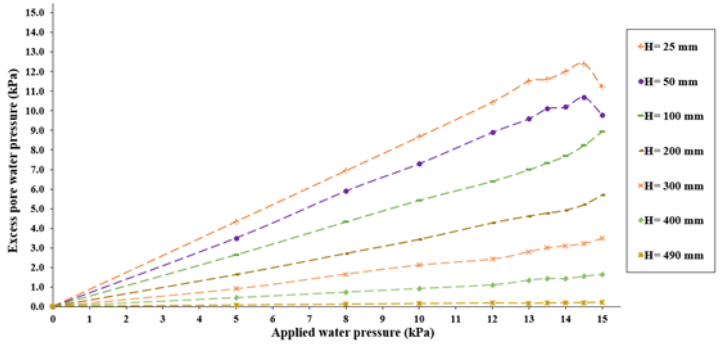

Figure 4: Excess of pore water pressure distribution after 2s of simulation at different heights (H) for a centred cross-section considering different applied pressures. Single-point MPM results.

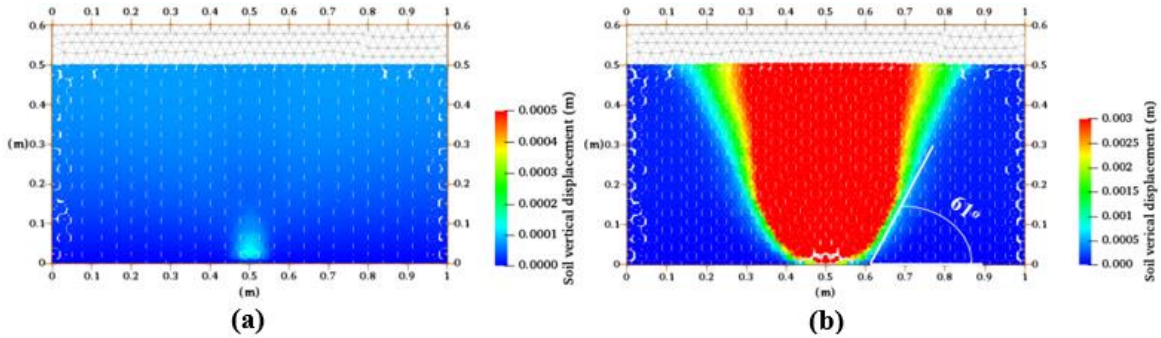

Figure 5: Soil vertical displacement after 2s of simulation in a submerged soil bed where an excess water pressure of (a) p=10 kPa or (b) p=14.5 kPa is imposed at the orifice.

When the applied pressure on the orifice is just beyond the pressure that triggers global fluidization (p=14.5-15 kPa), the MPM single-point calculation crashes before reaching quasistatic conditions. Figure 6 shows the vertical displacement distribution just before the calculation terminates for p=16 kPa. The reason for this numerical instability is that during the uplift mechanism, MPs are dragged vertically through the computational mesh, and elements

near the orifice may become empty. This results in the formation of unrealistic voids within the continuum that affects the continuity of the stress and strain fields (Yerro, 2015). This situation with empty elements near the orifice also causes a disconnection between the boundary nodes (where the pressure p is applied) and the actual soil, which means that the applied pressure will not dissipate into the soil bed. This numerical issue has been previously addressed by the addition of virtual MPs (Beuth, 2012). Virtual MPs are integration points with negligible mass that are added in the empty elements to enhance the continuity of the solution.

However, there is another limitation of the current two-phase single-point model that prevents the calculation from proceeding after the fluidization onset. A unique linear elastic-perfectly plastic constitutive law (Mohr-Coulomb) is considered to describe the soil behavior. This is not realistic at the post fluidization stage when solid grains are not in contact and the soil has a liquid-like behavior. Therefore, the inability of the constitutive model to transition from 'solid-like' to 'liquid-like' behavior leads to the calculation to crash.

In the next section, the ability of the double-point approach to simulate the progression of the onset of fluidization is demonstrated.

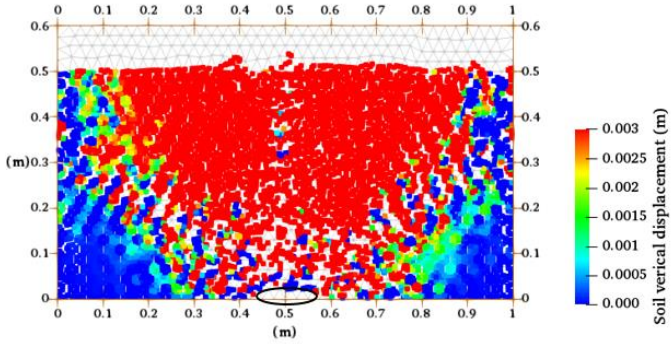

Figure 6: Soil vertical displacement during the post local fluidization mechanism in submerged soil bed where an excess water pressure of 16 kPa is imposed at the orifice.

4.2 Two-Phase Double-Point Results

In this section, the results obtained with the double-point approach are presented. The double-point approach distinguishes between solid-like and liquid-like behavior of the soil (represented by the SMPs) based on the maximum porosity value n_{max}. In order to visualize the state of the soil, Figure 7 shows the porosity field at the maximum development of fluidization for two different inflow velocities. Figure 7a considers an inflow velocity of 10^{-3} m/s, which is equivalent to a water pressure of 14.5 kPa that was identified as the pressure required for the onset of soil fluidization in the single-point simulation. In this case, the maximum porosity ($n_{max} = 0.45$) is only reached locally in the vicinity of the orifice, indicating that the fluidization starts but does not progress.

If the prescribed inflow velocity increases to 10^{-2} m/s, the fluidization mechanism progresses and reaches the surface. This can be seen in Figure 7b, where the porosity field is presented at the time of maximum fluidization. The liquid-like zone (represented by those SMPs with the maximum porosity) connects the orifice with the top of the model. At this point, the fluidized zone forms an inclined wedge-shaped failure surface that breakthrough the soil surface. Afterward, the fluidized zone is consequently dragged away by the LMPs flow along the soil surface.

The soil fluidization mechanism is associated with an uplift mechanism of the soil bed (due to the reduction in effective stress) above the pipe orifice (maximum of 80 mm), as shown in Figure 8. The prediction from the MPM simulation shows a good qualitative agreement with

the previous experimental study conducted by Alsaydalani (2010), who observed that the soil fluidization is attributed to an uplift mechanism of the grains in the fluidized region of the soil. These results show the two-phase double-point MPM formulation's capability in identifying the soil fluidization mechanism induced by a leaking pressurized water pipe.

A key consideration in this paper is the limitations of the double-point MPM approach. While these limitations have not had a significant impact on the overall scope of the paper and meeting its objectives, they have affected the findings of the study to a certain extent. Some of these limitations include but are not limited to numerical instabilities, originated due to grid crossing and volumetric locking. These instabilities affect the accuracy of the results, including the pore pressure distribution in water. Thus, a proper strategy needs to be identified in the extension of this study. Also, the possibility of having artificially dry elements in the saturated soil can create spurious oscillations. The latest can be solved by increasing the number of SMPs.

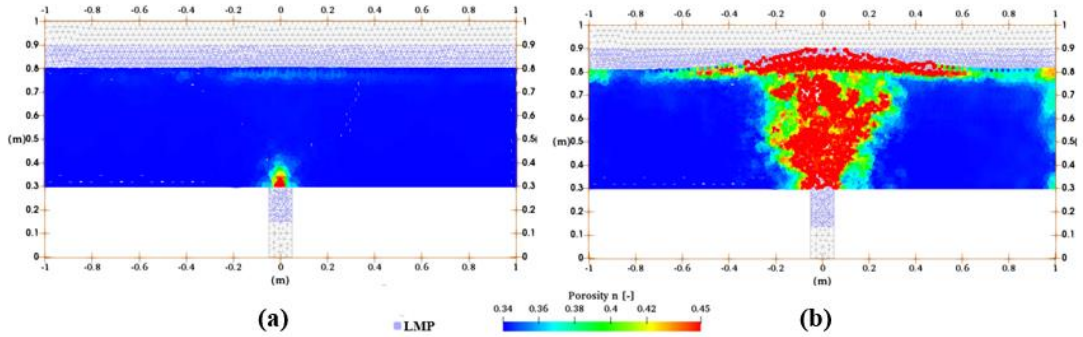

Figure 7: Soil porosity after 2s of simulation at the SMPs (a) at the onset of fluidization considering an inflow of 10^{-3} m/s and (b) when the fluidization reaches the surface considering an inflow velocity of 10^{-2} m/s. The LMPs are also represented with little blue dots.

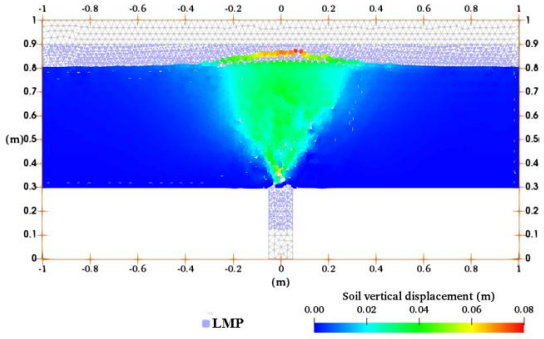

Figure 8: Soil vertical displacement after 2s of simulation at the SMPs when fluidization reaches the surface (inflow velocity of 10^{-2} m/s). The LMPs are also represented with little blue dots.

5. CONCLUSIONS

This paper demonstrates and compares the capabilities of the two-phase single-point and double-point MPM formulations to simulate the onset and evolution of soil fluidization associated with a leaking buried pressurized water pipe embedded in fully saturated sand. The results show that the single-point formulation is applicable for identifying the leak pressure required for the initiation of the local fluidization in the vicinity of the orifice. However, it is not capable of capturing post-local fluidization mechanism due to the formation of empty elements near the orifice and the inability of the constitutive model to represent the transition

from solid-like to liquid-like behavior. The two-phase double-point MPM formulation, together with the use of in/outflow boundary conditions, can capture the evolution of soil fluidization around a leaking pipe until it reaches the soil surface. The MPM results demonstrate how the vertical soil displacements, excess pore water pressures, and porosity develop during the onset of fluidization and post fluidization. It can be observed that the excess pore water pressures close to the orifice drop at the onset of fluidization. Future work is needed to address numerical instabilities, including the grid crossing and the volumetric locking. In general, the results are qualitatively consistent with previous experimental and numerical works. The double-point MPM formulation will be further developed for this application to study the effect of the crack size in the soil fluidization mechanism around a leaking pipe. It is worth mentioning that the fluidization mechanism captured by the porosity threshold is also limited by the assumption that the liquid-like response of the soil is Newtonian. Further work needs to be carried out to investigate the impact of this assumption.

REFERENCES

Al-Kafaji, I. K. J. (2013) *Formulation of a Dynamic Material Point Method (MPM) for Geomechanical Problems.* Ph.D. Thesis. Univ. of Stuttgart.

Alsaydalani, M.O.A. (2010) *Internal fluidization of granular material*. Ph.D. Thesis. Univ. of Southampton.

Anura3D (2021) *Anura3D-MPM Research Community.* Available at: www.anura3D.com

Bandara S. and Soga K. (2015) 'Coupling of soil deformation and por-e fluid ow using material point method', *Computers and Geotechnics*, 63, pp. 199-214.

Bear, J. (1972) *Dynamics of fluids in porous media.* New York: Elsevier.

Beuth, L. (2012) *Formulation and application of a quasi-static material point method.* Ph.D. Thesis. Univ. of Stuttgart.

Biot, M.A. (1941) 'General theory of three-dimensional consolidation', *Journal of applied physics*, 12 (2), pp. 155-164.

Beenakker, C.W.J. (1984) 'The effective viscosity of a concentrated suspension of spheres (and its relation to diffusion)', *Physica*, 128, pp. 48–81.

Ceccato, F., Beuth, L. and Simonini, P. (2016) 'Analysis of piezocone penetration under different drainage conditions with the two-phase material point method', *Journal of Geotechnical and Geoenvironmental Engineering*, 142 (12), p. 04016066.

Ceccato, F., Yerro, A. and Martinelli, M. (2018) 'Modelling soil-water interaction with the material point method. Evaluation of single-point and double-point formulations', In *Numerical Methods in Geotechnical Engineering IX, Proceedings of the 9th European Conference on Numerical Methods in Geotechnical Engineering*, 25-27 June. Porto, Portugal. CRC Press.

Colombo, A.F., and Karney, B.W. (2002) 'Energy and Costs of Leaky Pipes: Toward Comprehensive Picture', *Journal of Water Resources Planning and Management*, 128 (6), pp. 441-450.

Cui, X. (2013) *Numerical simulation of internal fluidization and cavity evolution due to a leaking pipe using the coupled DEM-LBM technique*. Ph.D. Thesis. Univ. of Birmingham.

Global Water Leakage Summit (2008) 'Adapting the Most Effective Strategies for Water Efficiency and Leakage Management'. *Proceedings of the 3rd Annual Leakage Summit for International Water Utilities*, London, UK.

Li, J. (2013) *Numerical investigations of the coupled DEM-LBM technique with application to leakage-soil interaction due to a leaking pipe*. Ph.D. Thesis. Univ. of Birmingham.

Martinelli, M. (2016) 'Soil-water interaction with material point method. double-point formulation', *Report on EU-FP7 research project MPM-Dredge PIAP-GA-2012 324522*.

Martinelli, M. and Rohe, A. (2015) 'Modelling fluidization and sedimentation using material point method', *In 1st Pan-American Congress on Computational Mechanics.* Buenos Aires, Argentinia.

Phuong, N., van Tol, A., Elkadi, A. and Rohe, A. (2014) 'Modelling of pile installation using the material point method (MPM)', *Numerical Methods in Geotechnical Engineering*, 271, pp. 271-276.

Richards Jr, R., Elms, D.G. and Budhu, M. (1990) 'Dynamic fluidization of soils', *Journal of Geotechnical Engineering*, 116 (5), pp. 740-759.

Rogers, C.D.F., Chapman, D.N., and Royal, A.C.D. (2008) 'Experimental investigation of the effects of soil properties on leakage: final report [R]', *Report prepared for Thames Water Limited and Three Valleys Water Limited.* Univ. of Birmingham.

Soga, K., Alonso, E., Yerro, A., Kumar, K. and Bandara, S. (2016) 'Trends in large-deformation analysis of landslide mass movements with particular emphasis on the material point method', *Géotechnique*, 66 (3), pp. 248-273.

Sulsky, D., Chen, Z. and Schreyer, H.L. (1994) 'A particle method for history-dependent materials', *Computer methods in applied mechanics and engineering*, 118 (1-2), pp. 179-196.

Teeluckdharry, S. (2017) *An experimental investigation of leakage flow paths in soil surrounding leaks in water distribution systems*. Ph.D. Thesis. Univ. of Cape Town.

Truesdell, C. and Toupin, R. (1960) 'The classical field theories', In *Principles of classical mechanics and field theory/Prinzipien der Klassischen Mechanik und Feldtheorie*. Springer, Berlin, Heidelberg.

van Zyl, J.E., CGeol, F.G.S., and BIng, A.D. (2013) 'Soil fluidization outside leaks in water distribution pipes-preliminary observations', *Proceedings of the Institution of Civil Engineers*, 166 (10), pp. 546.

Wang, D., Bienen, B., Nazem, M., Tian, Y., Zheng, J., Pucker, T. and Randolph, M.F. (2015) 'Large deformation finite element analyses in geotechnical engineering', *Computers and Geotechnics*, 65, pp. 104–114.

Więckowski, Z. (2003) 'Modelling of silo discharge and filling problems by the material point method', *Task Quarterly*, 4 (4), pp. 701-721.

Yerro, A, Alonso, E and Pinyol, N (2014) 'Modelling progressive failure with MPM', In *Numerical Methods in Geotechnical Engineering.* Balkema, Leiden. The Netherlands, pp. 319–323.

Yerro, A. (2015) *MPM modelling of landslides in brittle and unsaturated soils.* Ph.D. Thesis. Univ. Politècnica de Catalunya.

Zabala, F. and Alonso, E.E. (2011) 'Progressive failure of Aznalcóllar dam using the material point method', *Géotechnique*, 61 (9), pp. 795-808.

Zhu, H., Zhang, L., Chen, C. and Chan, K. (2018) 'Three-dimensional modelling of water flow due to leakage from pressurized buried pipe', *Geomechanics and Engineering*, 16 (4), pp. 423-433.